Continental Shelf Research 29 (2009) 1289–1301

Contents lists available at ScienceDirect

Continental Shelf Research

journal homepage: www.elsevier.com/locate/csr

Modeling bio-geomorphological influences for offshore sandwaves

B.W. Borsje [a,b,*], M.B. de Vries [a,b,c], T.J. Bouma [d], G. Besio [e], S.J.M.H. Hulscher [a], P.M.J. Herman [d,f]

[a] Water Engineering and Management, University of Twente, P.O. Box 217, 7500 AE Enschede, The Netherlands
[b] Deltares, Marine and Coastal Systems, Rotterdamseweg 185, P.O. Box 177, 2600 MH Delft, The Netherlands
[c] Faculty of Civil Engineering and Geosciences, Delft University of Technology, P.O. Box 5048, 2600 GA Delft, The Netherlands
[d] Centre for Estuarine and Marine Ecology, Netherlands Institute of Ecology (NIOO-KNAW), Korringaweg 7, P.O. Box 140, 4400 AC Yerseke, The Netherlands
[e] Department of Civil, Environmental and Architectural Engineering, University of Genoa, Via Montallegro 1, 16145 Genoa, Italy
[f] Faculty of Environmental Sciences, Radboud University Nijmegen, P.O. Box 9102, 6500 HC Nijmegen, The Netherlands

ARTICLE INFO

Article history:
Received 22 October 2008
Received in revised form
16 February 2009
Accepted 22 February 2009
Available online 3 March 2009

Keywords:
Morphological/morphodynamic modeling
Sandwaves
Benthos
Stability analysis
Biogeomorphology
North Sea

ABSTRACT

The coastal environment shows a wide range of bed patterns, for which sandwaves and sandbanks are among the most common. Less known in this context is the high benthic diversity in the coastal environment, which gives rise to the question to what extend the benthos interacts with the shape of the seabed. This paper reviews field and flume experiments on bio-geomorphological influences between benthos and sediment and tests the hypothesis that both the occurrence and the dimensions of sandwaves are dependent on the benthic diversity in the North Sea. Mathematical inclusions to account for biological activity in idealized models reveal that biota is able to influence the wavelength of sandwaves significantly, compared to the default case. More importantly, the models indicate that biota is able to induce bed patterns under conditions when the physical parameters suggest a stable flat bed and vice versa. Present model explorations indicate that future research should focus on the parameterization of subtidal biological activity on sediment dynamics and thereby on seabed patterns. Such knowledge will enable process-based modeling of the spatial and temporal variation in biological activity on seabed morphodynamics and validate the proposed modeling approach with field measurements.

1. Introduction

Coastal areas are highly important both from an ecological and economical perspective, as these areas serve both for a broad variety of human activities and form the habitat for a broad variety of organisms. Many human activities such as offshore constructions, maintaining navigation channels and constructing pipelines and telecommunication cables depend on a good understanding of sediment dynamics in coastal waters (Németh et al., 2003). The conservation and management of the benthic biodiversity in the coastal zone also requires knowledge about spatial and temporal distribution of macrobenthic species and thus the sediment dynamics (Borja et al., 2000). Hence there is both from an ecological and economical perspective a growing interest in the biophysical interactions between benthos and their sedimentary environment. Studies from intertidal areas indicate that benthos can strongly influence local sediment composition and dynamics, by acting as either stabilizers or destabilizers (e.g. Widdows and Brinsley, 2002). The subtidal seabed is neither flat nor static, and significant differences can be found in the benthic assemblage related to meso-scale bedforms at the subtidal seabed (e.g., Baptist et al., 2006). Nevertheless, the feedback effects from these assemblages to the characteristics of the subtidal bedforms have not yet been studied.

Nowadays, idealized models are often used to predict seabed dynamics (for an overview see Besio et al., 2008). However, the hydrodynamics and sediment dynamics in these models lack correction for biological activity. Given the predictive power of the idealized models, extending the models with biological activity will give us a tool to better manage the utilization and conservation of the seabed.

The aim of this paper is (1) to explore the influences of biota on bedforms in a subtidal environment and (2) to propose formulations to include bio-geomorphological influences in idealized models. We will achieve these objectives by reviewing the offshore environment both from a morphodynamic and biological perspective (Section 2) and from the known impact of some key benthic species in the subtidal environment on the hydrodynamics and sediment dynamics (Section 3). We subsequently focus on methods to model such bio-geomorphological influences

* Corresponding author at: Water Engineering and Management, University of Twente, P.O. Box 217, 7500 AE Enschede, The Netherlands. Tel.: +31 53 489 3546; fax: +31 53 489 5377.
E-mail addresses: b.w.borsje@utwente.nl (B.W. Borsje), mindert.devries@deltares.nl (M.B. de Vries), t.bouma@nioo.knaw.nl (T.J. Bouma), giospud@dicat.unige.it (G. Besio), s.j.m.h.hulscher@utwente.nl (S.J.M.H. Hulscher), p.herman@nioo.knaw.nl (P.M.J. Herman).

0278-4343/$ - see front matter © 2009 Elsevier Ltd. All rights reserved.
doi:10.1016/j.csr.2009.02.008

List of symbols

Δ_r^*	ripple height, m
ϕ_0	local latitude, deg
ζ	dimensionless water depth
θ_{cr}	critical Shields parameter
θ_x,θ_y	Shields parameter in x and y direction
ρ^*	density of water, kg m^{-3}
ρ_s^*	density of sediment, kg m^{-3}
σ^*	angular frequency of the tide, rad s^{-1}
τ_x^*, τ_y^*	bed shear stress in x and y direction, Pa
ν^*	kinematic viscosity of water, m^2 s^{-1}
ν_T^*	kinematic eddy viscosity, m^2 s^{-1}
$\mathbf{\Omega}^*$	angular velocity of the Earth's rotation, rad s^{-1}
c	dimensionless sediment concentration
c_a	dimensionless reference concentration
C	dimensionless friction factor
d	dimensionless grain size
d^*	grain size, mm
d_{50}^*	median grain size, mm
$\mathbf{D}^*$	rate of strain tensor
$f_{Echinocardium,stab}$	stabilizing factor for the median grain size
$f_{Lanice,stab}$	stabilizing factor for the ripple height
$f_{Tellina,destab}$	destabilizing factor for the critical bed shear stress
F	function to describe the vertical structure of the eddy viscosity
g^*	gravity acceleration, m s^{-2}
h	dimensionless water depth
h^*	local water depth, m
h_0^*	average water depth, m
H	Heaviside function
k	von Karman constant
p^*	pressure, Pa
q_{Bx},q_{By}	dimensionless bed-load transport in x and y direction
q_{Px},q_{Py}	dimensionless transport due to slope effects in x and y direction
q_{Sx},q_{Sy}	dimensionless suspended-sediment transport in x and y direction
q_{Tx},q_{Ty}	dimensionless total sediment transport in x and y direction
R_p	particle Reynolds number
$\mathbf{u}^*$	velocity vector in x, y and z direction, m s^{-1}
U_0^*	depth-averaged flow velocity, m s^{-1}
z_r^*	roughness height, m

between key benthic species and hydrodynamics plus sediment dynamics (Section 4). Next the main findings of this paper are discussed (Section 5), leading to important general conclusions (Section 6). In the present paper we use the Dutch part of the North Sea as an example, as it has been relatively well described with respect to bedforms and organisms (details in the next sections).

2. Offshore environment of the Dutch coast

The Dutch part of the North Sea covers roughly 57,000 km^2 with a maximum water depth of 70 m (Fig. 1A). Several bedforms are present on the offshore seabed (Fig. 1B), distinguishable by their wavelength, height, orientation with respect to the tidal current and their capability to migrate. Sandbanks (Fig. 1C) have wavelengths (distance between two crests) of a few kilometers and an amplitude of tens of meters. The orientation of the crests with respect to the principal direction of the tidal current is up to 40° anticlockwise in the Northern Hemisphere. There is no evidence that sandbanks move (Dyer and Huntley, 1999). Sandwaves (Fig. 1D) have much smaller wavelengths (of the order of hundreds of meters), while the heights are up to 5 m. Sandwaves migrate with a speed of tens of meters per year (McCave, 1971). Their orientation is almost perpendicular to the direction of the main current. Sandbanks are associated with relatively weak tidal currents, whereas sandwaves are related to strong tidal currents. As a result, sandbank and sandwave fields sometimes partly overlap.

The sandbanks and sandwaves occurring in the Dutch part of the North Sea differ in location (top panel Fig. 2, after Hulscher and Van den Brink, 2001), and together cover approximately 42% of the Dutch part of the North Sea. Combining the locations with maps showing the spatial distribution of physical properties like mud content (defined as the weight of the mud fraction divided by the weight of the total sample), median grain size, slope, current velocity and water depth (Fig. 3), it can be seen that the sandbanks and sandwaves clearly differ in some of their physical characteristics (Fig. 2 bottom panel). Non-surprisingly, the spatial analysis clearly shows that sandwaves do not occur in muddy environments.

The bottom of the North Sea is inhabited by a great number of benthic organisms that live in and on the bottom of the sea (Heip et al., 1992; Künitzer et al., 1992; Rabaut et al., 2007). By their activities these benthic organisms can modify their habitat, which is generally referred to as bio-geomorphological influence. The benthic community's composition on the seabed is generally related to physical parameters like median grain size, slope, mud content and water depth (e.g. Degraer et al., 2008). Consequently, we only focus on benthos existing in the parameter range presented in Fig. 2.

In the present paper, we focus on three species that are (1) characteristic for benthos living in sandwaves and sandbanks in the North Sea, (2) can be found in large amounts in and on the bed and (3) have significant influences on the surrounding environment. The first one is the sea urchin *Echinocardium cordatum* (Mortensen, 1927), which is usually 40–50 mm in length, has a density distribution of around 20 individuals m^{-2} and lives up to 200 mm deep into the sediment. The second species is the tube building worm *Lanice conchilega* (Holthe, 1986). The worm can reach a length of up to 150 mm, partly protruding from the sediment, and its density distribution is locally extremely large (over 3000 individuals m^{-2}). Finally, the third species we study is the clam *Tellina fabula* (Tebble, 1966), which has a maximum shell length of 20 mm, a slightly smaller density distribution compared to *E. cordatum* of around 15 individuals m^{-2} and lives up to 100 mm deep in the sediment.

The influence of these three species on the sediment dynamics and hydrodynamics will be compared to the default case, which is defined as the situation in which no biological activity is present.

3. Impact of subtidal biota on sediment dynamics and hydrodynamics

The interaction between biota and sediment dynamics has been well studied and clearly shown for the intertidal environment in field studies (e.g. Austen et al., 1999; De Deckere et al., 2001; Andersen et al., 2002), flume experiments (e.g. Widdows et al., 1998; Orvain et al., 2006; Van Duren et al., 2006) and modeling studies (e.g. Paarlberg et al., 2005; Lumborg et al., 2006; Borsje et al., 2008a). From these studies it has become evident

that the intertidal biota can influence the hydrodynamics in different ways, like adding roughness to the bottom (e.g., by mussels, Van Leeuwen et al., 2008), or flow deceleration within epibenthic structures (e.g., by vegetations, Bouma et al., 2007). Most importantly, all these studies conclude that biota is able to influence both the sediment dynamics and hydrodynamics by several orders of magnitude and can act on a large spatial (tidal basin) and temporal (seasonal and inter-annual) scale. Compared to the benthos biomass per unit area in intertidal systems, the benthos biomass in subtidal areas in the North Sea is much smaller. Nevertheless, some explorative studies already show that such relatively small benthic biomass can still influence the sediment dynamics significantly (e.g., Knaapen et al., 2003; Borsje et al., 2008b). We will now review the available research for three benthic species that are likely to be relevant for subtidal sandbanks and sandwaves: *E. cordatum, L. conchilega*, and *T. fabula.*

The sea urchin *E. cordatum* has been shown to displace up to 20,000 $cm^3\,m^{-2}\,d^{-1}$, causing all the surface sediment to be reworked about once every 3–4 days (Lohrer et al., 2005). Moreover, field experiments in the Gullmar Fjord (Western Sweden) show that the reworking intensity was directly related to the biovolume of the *E. cordatum* individuals (Gilbert et al., 2007). Being a surface deposit feeder, *E. cordatum* may rapidly transport particles from the sediment surface deeper into the sediment (Osinga et al., 1997), which results in a heterogeneous sediment distribution in the top centimeters of the bed (Fig. 4). Although *E. cordatum* is regarded as a non-selective deposit feeder (Lohrer et al., 2005), its feeding activity will for two reasons result in a top layer of the sediment that consists of relatively coarser particles, compared to the default case in the absence of benthos. Firstly, *E. cordatum* feeds on organic matter. Given that fine sediment is richer in organic matter, compared to coarse sediment (Burone et al., 2003), *E. cordatum* moves to a new spot after it has reworked all the fine sediment, leaving the coarser sediment particles that are not ingested at their original position on top of the sediment (Cramer et al., 1991). Secondly, the chance to get ingested and brought downward is larger for small particles relative to coarse particles, as finer particles have a relative larger surface area. A comparable non-selective deposit feeder (*Arenicola marina*), is able to double the grain size in the top five centimeters of the bed, compared to the case in which no *A. marina* was included, for an experiment with initially the same vertical sediment distribution (Baumfalk, 1979).

The tube building worm *L. conchilega*, is known to occur in high densities which have a decelerating effect on the near-bottom flow, and thereby cause fine particles to deposit within such patches (Eckman et al., 1981; Rabaut et al., 2007). Given both the lower near-bottom flow velocity and a smaller median grain size at the sediment surface compared to the default case in the absence of benthos, the ripples on top of the sediment surface are lower (Fig. 4), as observed in the field by Featherstone and Risk (1977). Such an effect is highly important, as ripples are the main origin of seabed roughness and one of the main determinants of the amount of sediment transported (Soulsby, 1983). Given the maximum density of *L. conchilega* found in the North Sea (3000 ind m^{-2}) the near-bottom velocity will reduce to 30% of the near-bottom flow, relative to the default case, according to the flume experiment by Friedrichs et al. (2000). Such flow reduction

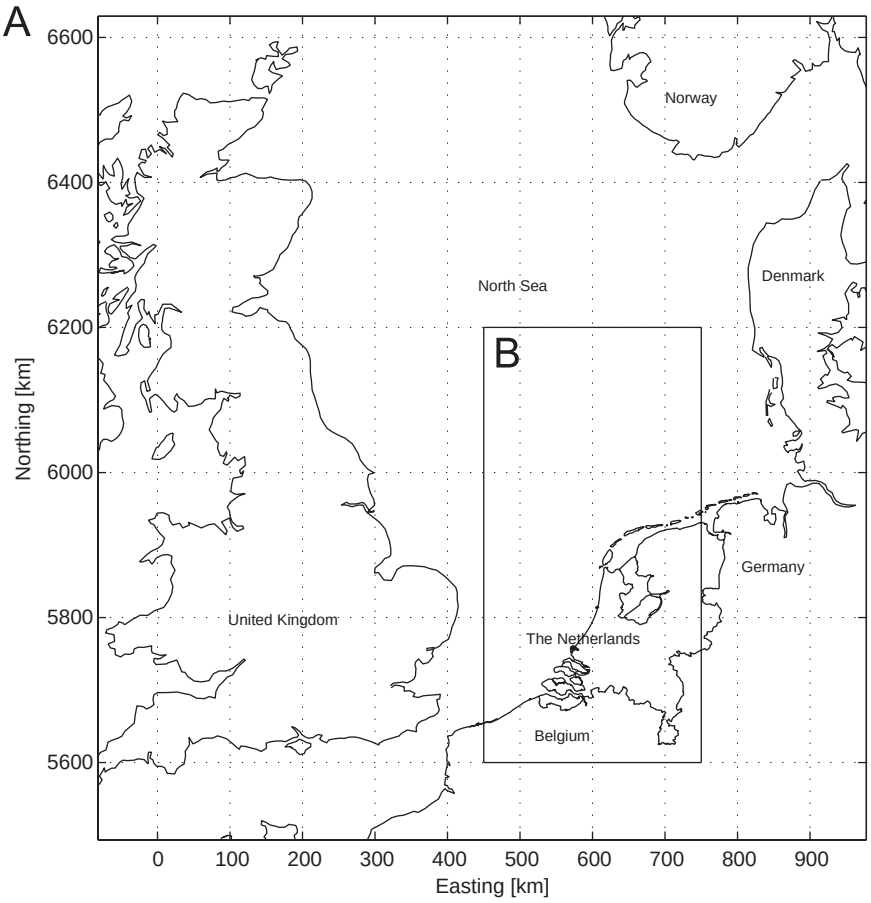

Fig. 1. Seabed patterns in the Dutch part of the North Sea (A, B), in which sandbanks (C) and sandwave fields (D) can be distinguished. Grid size is $200 \times 200\,m^2$.

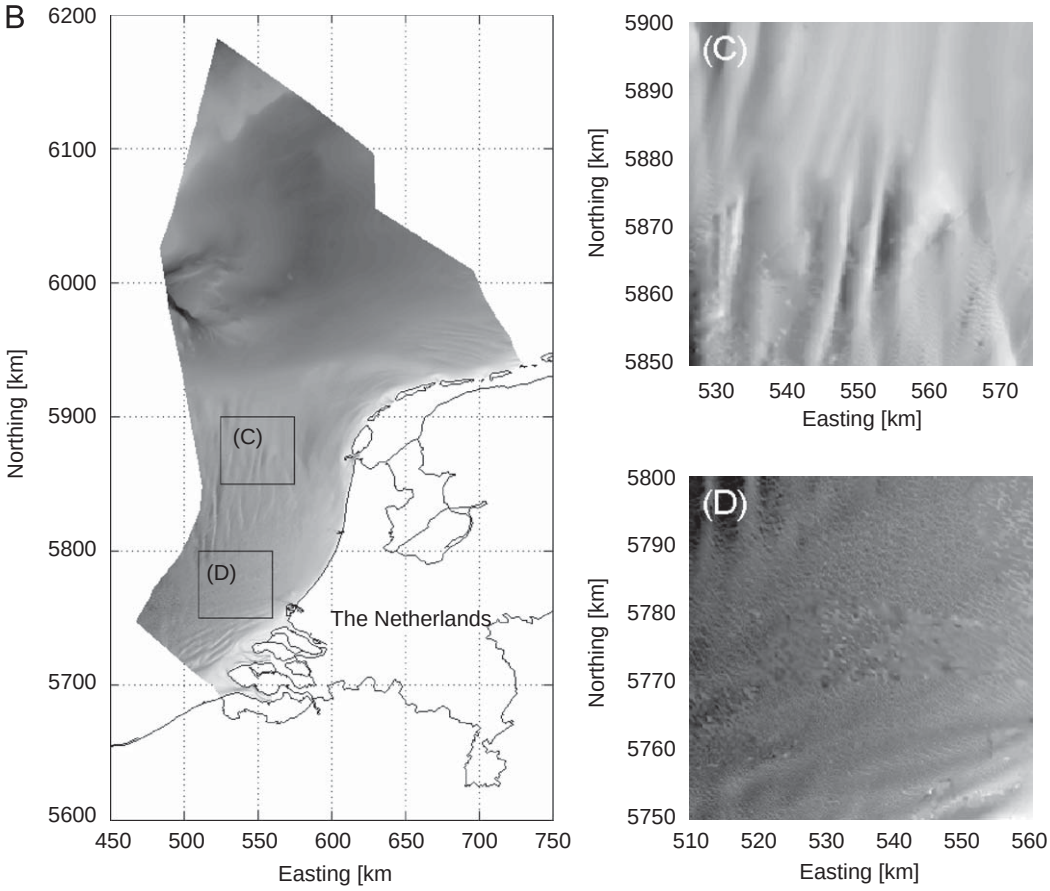

Fig. 1. (*Continued*)

will decrease the ripple height up to 70%, based on empirical relations given by O'Donoghue et al. (2006).

The bivalve *T. fabula* is a selective deposit feeder as well as a suspension feeder. Due to its burrowing and feeding activities, the surficial sediment structure is disturbed, making it more prone to erosion (Austen et al., 1999). Data on the bio-engineering capacity of the bivalve *T. fabula* are scarce, but the sediment modification by the bivalve *Macoma balthica* is much better known (e.g. Widdows et al., 2000). Whereas both bivalves have comparable feeding strategies, they occur in quite different sediment types. However, *M. balthica* is mostly found in muddy sediments, while *T. fabula* prefers fine sand. Therefore, the distribution of *M. balthica* is concentrated in muddy estuaries and bays, the Wadden Sea, and in a narrow zone along the coast, in contrast to *T. fabula* which can be found in all other parts of the North Sea. Based on field measurements, Borsje et al., (2008a) constructed a parameterization of the relation between the biomass of *M. balthica* and the critical bed shear stress. At low biomass, the grazers cause a large modification of the critical bed shear stress, whereas at high biomass the grazers will not further reduce the critical bed shear stress. In other words, for large biomass grazers, the critical bed shear stress is estimated to be about 60% compared to the critical bed shear stress for the default case.

4. Modeling the role of bio-geomorphological influences on seabed patterns

As first pointed out by Huthnance (1982), bed patterns associated with tides are often free instabilities of the seabed, originating from the interaction between the sandy seabed and the depth-averaged water motions induced by tide propagation. Hulscher (1996) elaborated on this idea, and found that sandwaves are generated by residual vertical circulation cells, whereby sediment at the bed is transported towards the crests. The occurrence of sandwaves and sandbanks can be reasonably fairly predicted for the North Sea in both a qualitative (Hulscher and Van den Brink, 2001) and quantitative way (Cherlet et al., 2007). The latter two studies used linear stability analysis to determine a specific wavelength and an orientation of the most unstable component of the bed perturbations, which can be assumed to coincide with the appearing bedform. For a detailed explanation on the theory behind the use of linear stability analysis for understanding morphodynamic behaviour of coastal systems see Dodd et al. (2003).

The model used in the present paper is based on the work by Besio et al. (2006) and later modified by Cherlet et al. (2007), who modeled sandwave lengths along the Belgium continental shelf. By linking the relations described in Section 3 with the idealized model of Cherlet et al. (2007), a first insight can be obtained into the possible influence of benthos on the wavelength and occurrence of offshore sandwaves.

In order to perform the linear stability analysis, firstly the flow field must be evaluated and secondly a predictor for the sediment transport rate needs to be imposed. The parameterization of biological activity on the hydrodynamics and sediment transport is discussed in Section 4.1. The results of the inclusion of bio-geomorphological influences in the model are subsequently discussed in Section 4.2. A detailed description of the used bio-sandwave model is included in Appendix A.

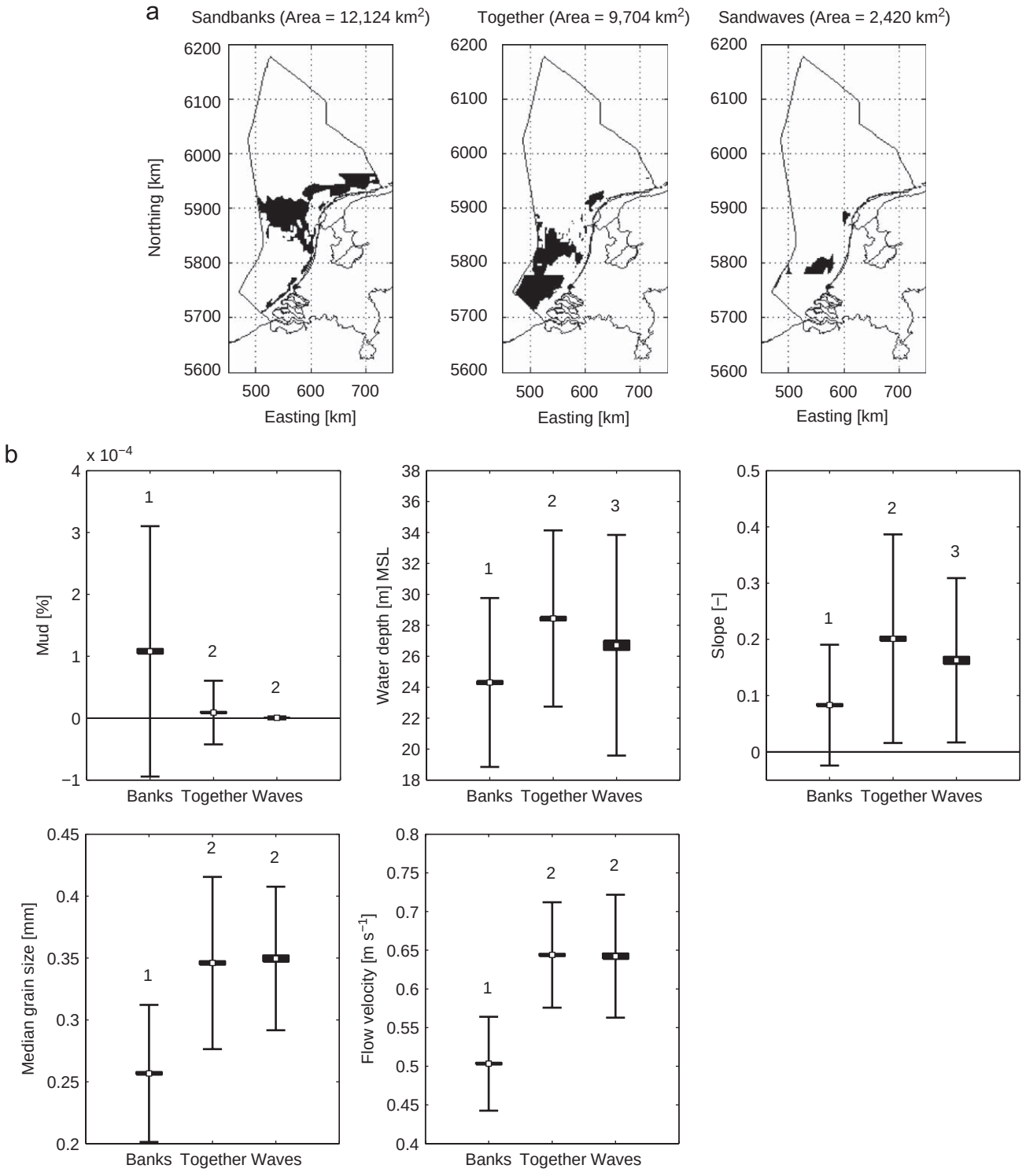

Fig. 2. Occurrence of sandbanks and sandwaves in the Dutch part of the North Sea and the relation to physical parameters. Mean, box: standard error, whiskers: standard deviation. Different numbers (1–3) point to significant differences among means (post hoc LSD test: $p_0 < 0.05$).

4.1. Parameterization of biological activity

Borsje et al. (2008b) suggested to quantifying the influence of the biological activity by *L. conchilega* by

$$\Delta_r^* = \Delta_r^{*0} f_{Lanice,stab}, \quad (1)$$

where $f_{Lanice,stab}$ is the biological factor for the ripple height (Δ_r^*). The superscript '0' for the ripple height represents the value without the influence of biological activity (default). A star denotes dimensional quantities. The biological factor is dependent on the abundance of *L. conchilega.* As discussed in Section 3, the minimum value for $f_{Lanice,stab}$ for the North Sea area is 0.3.

By adopting a representative North Sea case (water depth = 25 m; grain size = 0.3 mm; flow velocity = 0.6 m s^{-1}; Fig. 2) and reducing the ripple height to 30%, the eddy viscosity profile shows a clear biological influence compared to the physical case without

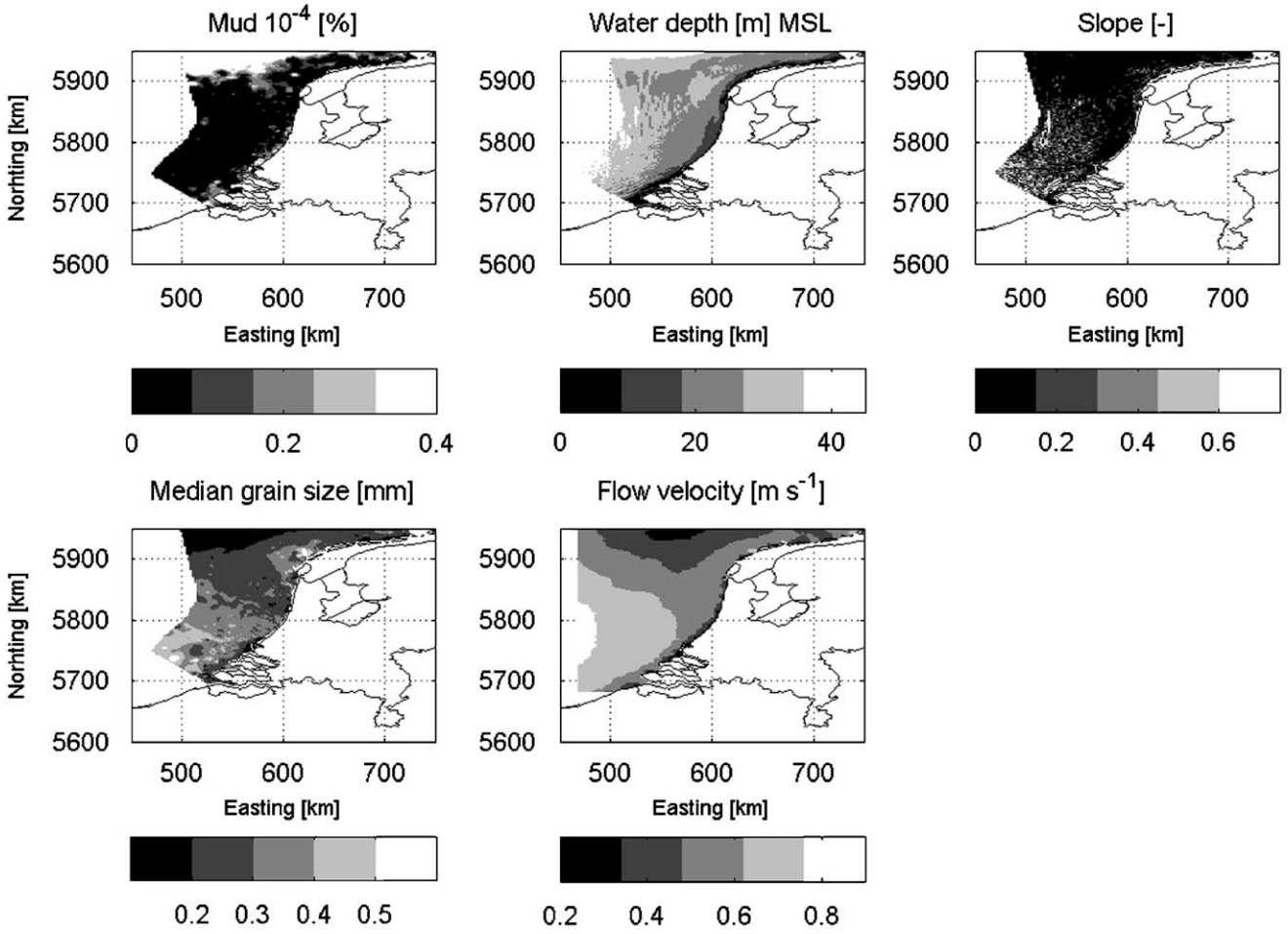

Fig. 3. Spatial distribution of the physical parameters, focusing on the area of interest (see Fig. 2 top panels). Grid size is $2 \times 2\,km^2$, resulting in nearly 15,000 grid cells for the Dutch part of the North Sea.

biology (Fig. 5). For the given parameter settings, the default ripple height Δ_r^{*0} is 20 mm. However, the *L. conchilega* abundance will reduce the ripple height Δ_r^* to 6 mm. The corresponding lower eddy viscosity causes both lower suspended-sediment concentrations and lower bed-load transport rates, compared to the default case that does not include biological effects. In relative terms, the decrease in suspended-load transport is large compared to the decrease in bed-load transport, as the eddy viscosity is mainly influenced in the suspended-load region, and not close to the bed, where the bed-load transport takes place. Moreover, a lowering of the ripple height is related to a lowering of the bed shear stress, resulting in lower bed-load transport rates and suspended-sediment concentrations, compared to the default case. Accordingly, the wavelength of the sandwaves will become smaller compared to the default case.

Similar to the biological influence by *L. conchilega* (Section 4.1), the influence of the biological activity by *T. fabula* and *E. cordatum* can be quantified by

$$\theta_{cr} = \theta_{cr}^{0} f_{Tellina,destab}, \tag{2}$$

$$d_{50}^{*} = d_{50}^{*0} f_{Echinocardium,stab}, \tag{3}$$

where $f_{Tellina,destab}$ and $f_{Echinocardium,stab}$ are the (de)stabilizing biological factors for the critical bed shear stress and grain size, respectively, θ_{cr} is the critical Shields parameter below which no sediment moves and d_{50}^{*} is the median grain size. Again, the superscript '0' for the critical bed shear stress and the median grain size represent the values without the influence of biological activity (default). The biological factor is dependent on the abundance of *T. fabula* and *E. cordatum*. As discussed in Section 3, the minimum value for $f_{Tellina,destab}$ for the Dutch part of the North Sea area is 0.6, while the maximum value for $f_{Echinocardium,stab}$ is 2.

Burrowing and grazing activities by *T. fabula* cause a decrease in critical bed shear stress. Consequently, both the bed-load and suspended-load transport will increase. The exact influence on the wavelength of sandwaves is difficult to predict, since the contribution of both transport modes to the sandwave length depends on the physical conditions. For low flow velocities, the suspended load is small, and bed-load transport rates will be relatively higher compared to the default case, due to the decrease in critical bed shear stress. Consequently, the wavelength of sandwaves will be smaller, relative to the default case. However, for higher flow velocities, the rate of suspended load becomes important and its presence provides a stabilizing contribution to the process leading to sandwave formation. As a result, the wavelength of sandwaves will be longer, compared to the default case.

E. cordatum redistributes the sediment, resulting in a larger median grain size at the sediment–water interface, compared to the default case. First of all, the bed-load and suspended-load transport will decrease, due to the larger grain size and consequently larger critical bed shear stress. Moreover, an

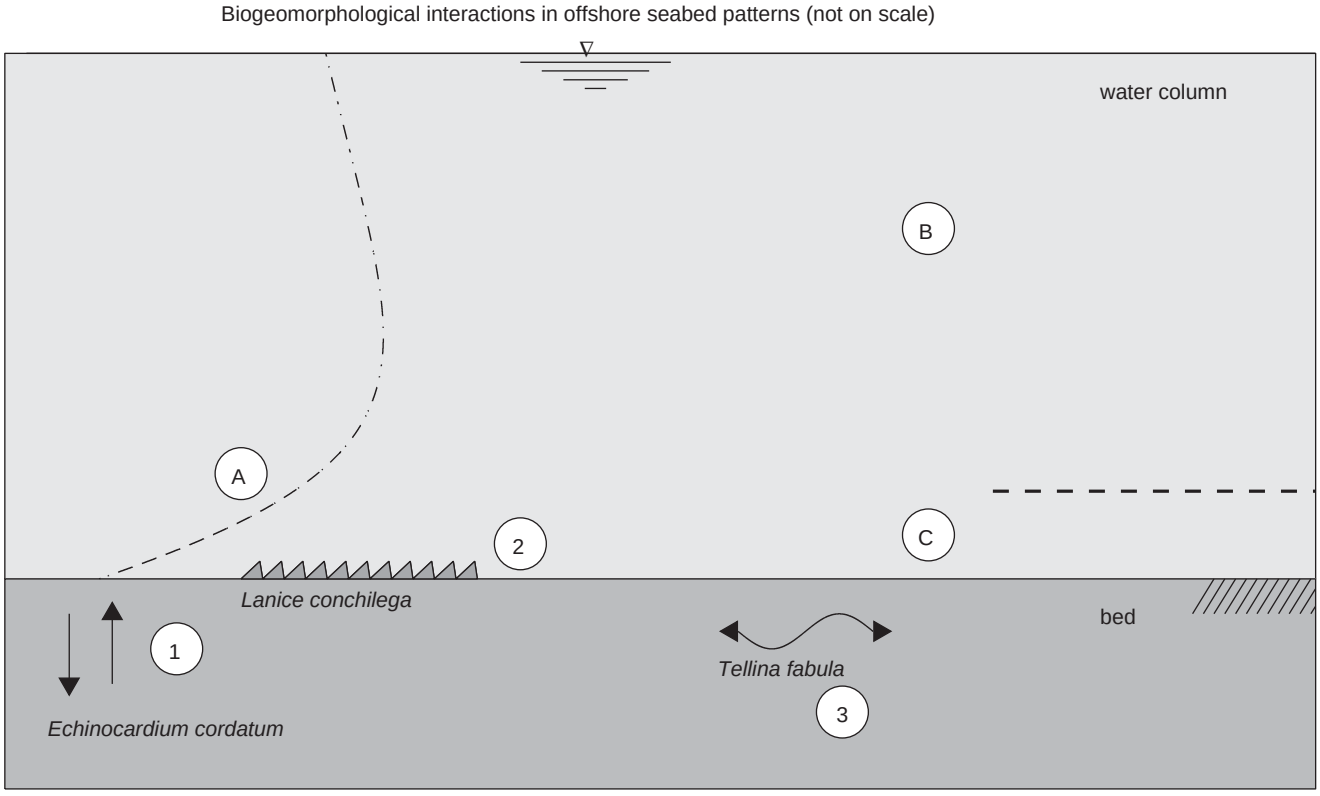

Fig. 4. Schematic overview of the bio-geomorphological influences (1–3) by *Echinocardium cordatum*, *Lanice conchilega* and *Tellina fabula*, and the consequences for the sediment dynamics and hydrodynamics (A–C), which will be discussed in Section 4.

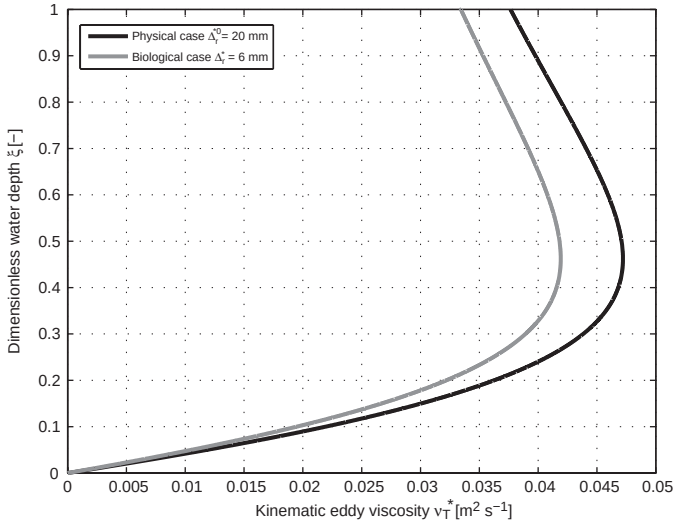

Fig. 5. Kinematic eddy viscosity (υ^*_T) plotted against dimensionless water depth (ζ) for the physical case and the case in which biological activity by *Lanice conchilega* is included. Kinematic eddy viscosity profile is shown for a typical North Sea case: water depth $h^*_0 = 25$ m, grain size $d^* = 0.3$ mm and flow velocity is $U^*_0 = 0.6\,\mathrm{m\,s^{-1}}$. Consequently, the ripple height in the default case (Δ_r^{*0}) is much larger compared to the biological case (Δ_r^*).

Table 1
Range of process parameters used in the idealized bio-sandwave model for the local water depth (h_0^*), grain size (d^*) and flow velocity (U_0^*).

	Mean	Minimum	Maximum
h_0^* (m)	30	20	40
d^* (mm)	0.35	0.2	0.5
U_0^* ($\mathrm{m\,s^{-1}}$)	0.65	0.5	0.8
Tellina fabula	–	–	$\theta_{cr} = 0.6\theta_{cr}{}^0$
Lanice conchilega	–	–	$\Delta^*{}_r = 0.3\Delta^*{}_r{}^0$
Echinocardium cordatum	–	–	$d^* = 2d^{*0}$

Moreover, the maximum biological influence for the three different bio-engineers is quantified. The superscript '0' for the critical bed shear stress (θ^*_{cr}), ripple height (Δ^*_r) and grain size (d^*) represent the value without the influence of biological activity (default).

increase in grain size will result in a higher roughness height, and therefore higher bed shear stresses. In contrast, a lower roughness height is induced by *L. conchilega*. In summary, the overall effect of different types of biota on the sandwave length is difficult to predict, given the various influences on the different model parameters. Therefore, including the extreme biological factors in the idealized model (Cherlet et al., 2007) is valuable to give some insight into the possible influence biota have on the sandwave length and sandwave occurrence.

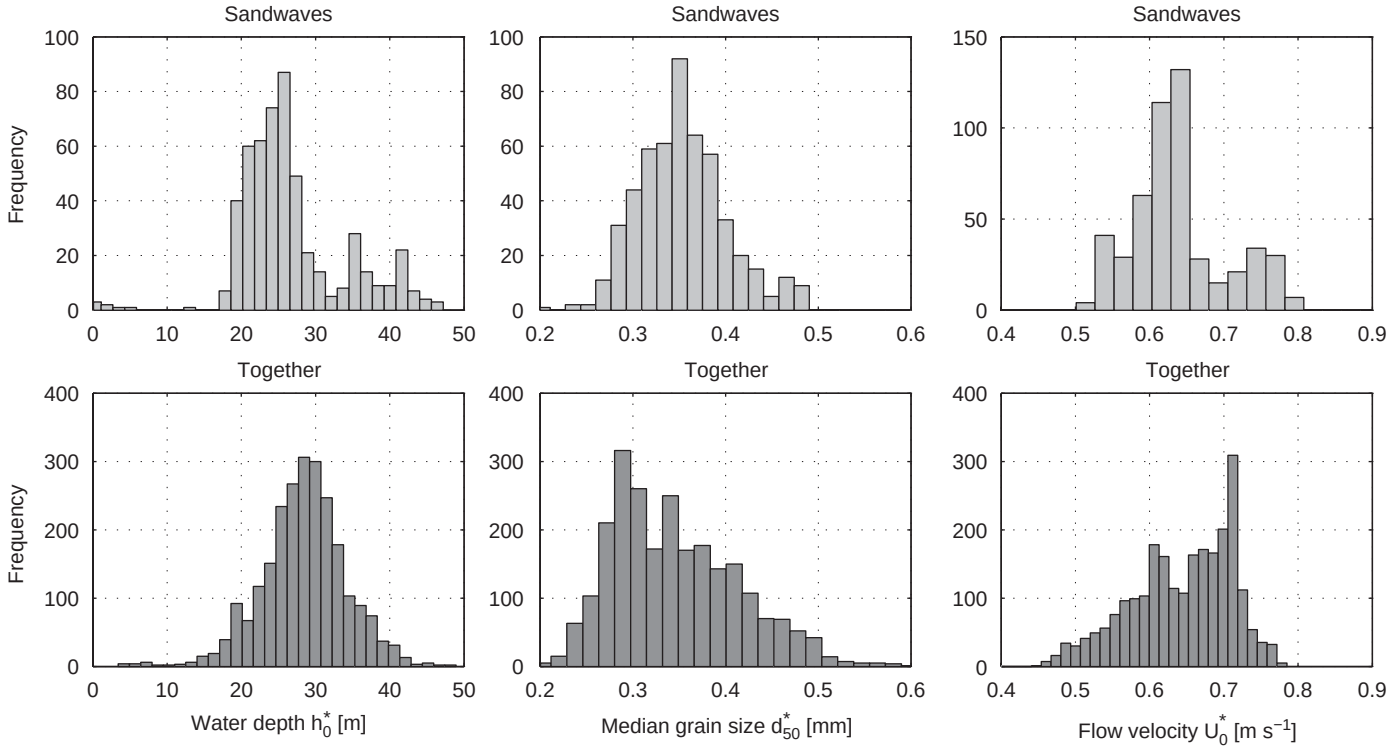

Fig. 6. Histograms plots for water depth (h^*_0), median grain size (d^*_{50}) and flow velocity (U^*_0). Distinction between areas where sandwaves occur (top panels) and areas where both sandwaves and sandbanks occur (lower panels), for reference see Fig. 2.

4.2. Modeling results

The model is run for two different cases: using the default parameter settings without including biological activity (default case) and a case in which the transport parameters are modified by the presence of biological activity (biological case). All model parameters are listed in Table 1. The range in model parameters is based on the histogram plots for the water depth, flow velocity and median grain size (Fig. 6). Fig. 7 shows the wavelength for both cases in which two of the process parameters are kept constant (mean), and the third process parameter is varied according to the range shown in Table 1.

The results for the default case are in accordance with the results discussed by Borsje et al. (2008b), and are only discussed briefly hereafter. By increasing the water depth (left panels Fig. 7), the wavelength for the sandwaves in the default case grow almost linearly. This observation is the result of a decrease in the Shields parameter for an increase of water depth, causing lower transport rates and resulting in longer sandwaves (Besio et al., 2006). By increasing the median grain size (middle panels Fig. 7) the default model results first in a shorter wavelength. This reduction in wavelength is caused by a decrease in suspended-sediment concentrations for increasing grain sizes, since the presence of suspended sediment tends to increase the wavelength of sandwaves. However, once a critical grain size threshold is passed (i.e., d^*_{50} around 0.45 mm), the wavelength of the sandwaves increase strongly with grain size, as sediment is only transported as bed load (middle panels Fig. 7).

Finally, an increase in flow velocity (right panels Fig. 7) causes a decrease in wavelength, indicating that stronger tidal currents tend to generate shorter sandwaves. However, the wavelength of the sandwaves does reach a minimum. The latter may be explained that in case of very strong tidal currents, the suspended sediment provides a stabilizing mechanism, resulting in sandwaves with an almost constant wavelength.

The results for the biological case show a clear difference, compared to the default case. *E. cordatum* initiated longer sandwaves compared to the physical case. For almost all other model settings, less sediment is transported as both bed load and suspended load in the case for which *E. cordatum* is included, resulting in longer sandwaves. The contradiction for small grain sizes is due to the fact that small grain sizes are related to high suspended-sediment concentrations and therefore to longer sandwaves. However, due to the presence of *E. cordatum* the suspended-sediment concentrations for small grain sizes are significantly lower, because the grain size at the bed–water interface is doubled. Consequently, the wavelength for this typical model settings is smaller, compared to the default case.

The influence of *L. conchilega* is clearly opposite to the effect of *E. cordatum*, as *L. conchilega* causes sandwaves to become shorter compared to the physical case (Fig. 7). The main difference for the case in which *L. conchilega* is included relative to the case in which *E. cordatum* is included, is that the former species follows almost the same trend compared to the physical case, whereas the latter species is able to influence both the position and the trend of the line compared to the physical case.

The effect of *T. fabula* on the wavelength of the sandwaves is limited for current model parameter settings. As discussed before, *T. fabula* is only influencing the critical bed shear stress. Consequently, in the case where sediment transport is already present, as was the case for our model, *T. fabula* is hardly influencing the amount of bed-load or suspended-load transport, and therefore of limited influence on the wavelength of the sandwaves (Fig. 7). However, in those physical cases where hardly any sediment transport is initiated, *T. fabula* is able to have a significant influence on the wavelength of sandwaves, as shown by Borsje et al. (2008b) for the Belgium Continental Shelf.

We subsequently modeled sandwaves at three locations in the North Sea, which were selected based on their contrasting process

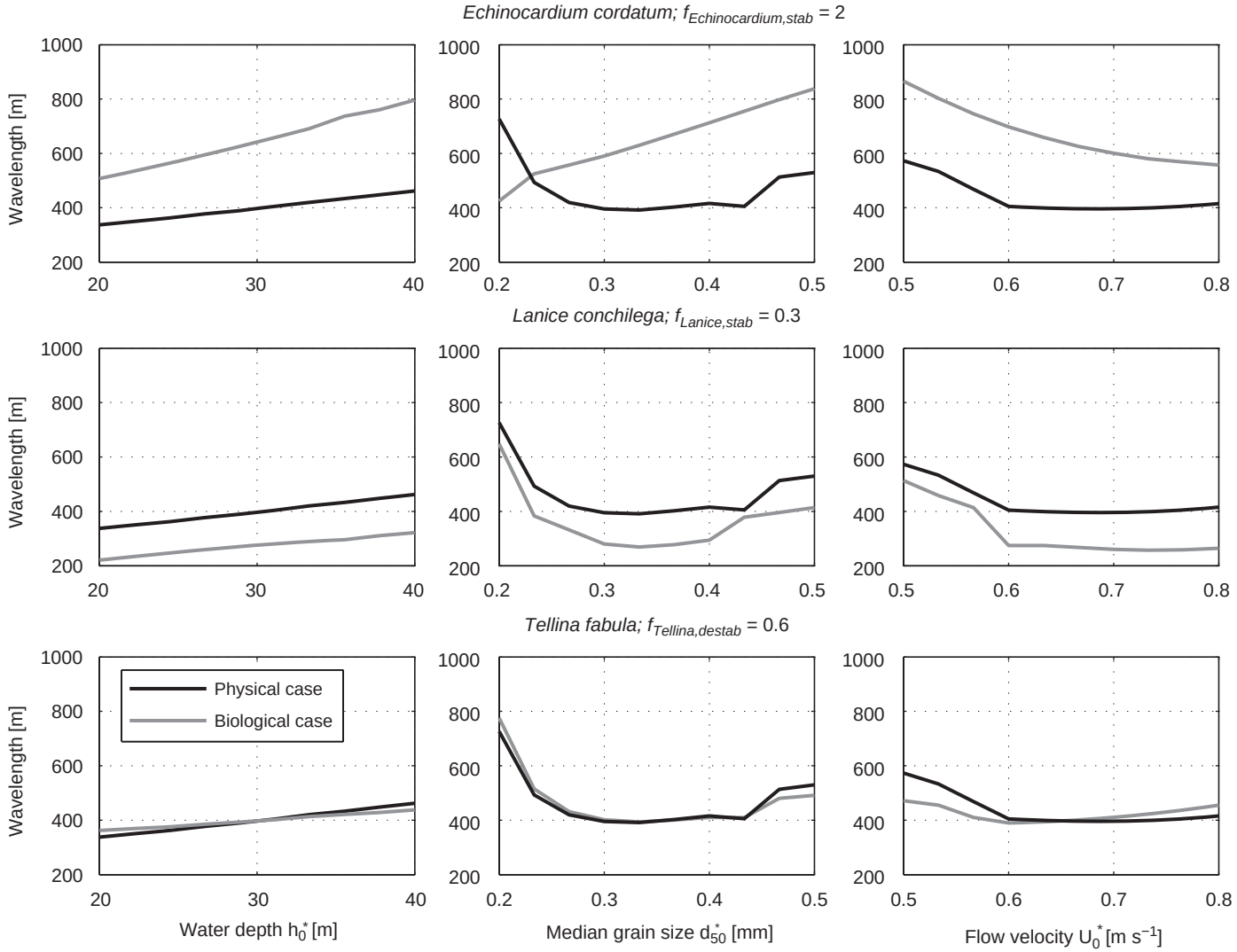

Fig. 7. Model results for the physical case (black line) and biological case (gray line), for the three different bio-engineers (rows), and variation in the three different process parameters (columns). For reference see Table 1.

parameters (Table 2). For every location, the model could give three distinctive outcomes. First, sandwaves are modeled with a certain wavelength (bars in Fig. 8). Secondly, no sediment transport is initiated (squares in Fig. 8). Finally, in some cases the bed turns out to be stable and flat due to the stabilizing effect of suspended sediment (triangles in Fig. 8). Location 1 is characterized by a high flow velocity, small grain size and a moderate water depth. As a result, suspended-sediment concentrations are high, resulting in a stable flat bed. However, due to presence of *E. cordatum* the grain size at the sediment–water interface is larger, relatively to the default case. This higher grain size results in lower suspended-sediment concentrations, and therefore a less destabilizing effect on the bed. Consequently the presence of *E. cordatum* allows the triggering of the formation of a wavy bed pattern, while in all other cases the bed is flat. Location 2 only differs from location 1 by having a much smaller water depth and a slightly larger median grain size. Similar to what we found for location 1, in most cases, the bed at location 2 also turns out to be a stable flat bed. The model however predicts that, *L. conchilega* is able to reduce the ripple height, and thereby preserving a wavy bed pattern. Finally, location 3 is characterized by a large water depth, and both a moderate flow velocity and grain size. In most cases, sediment is transported and sandwaves appear. However, the model indicates that at this location, *E. cordatum* will increase the grain size of the bed material and as a consequence, the sediment will not be transported.

Table 2
Model settings for the local water depth (h_0^*), grain size (d^*) and flow velocity (U_0^*), used to construct Fig. 8.

	Location 1	Location 2	Location 3
h_0^* (m)	25	5	40
d^* (mm)	0.2	0.3	0.5
U_0^* (m s^{-1})	0.8	0.8	0.5

Based on these model simulations, we conclude that bio-engineers can influence both the wavelength and the presence of bedforms significantly.

5. Discussion

This paper explores the bio-geomorphological influences in offshore seabed patterns, using a model analysis of the interaction

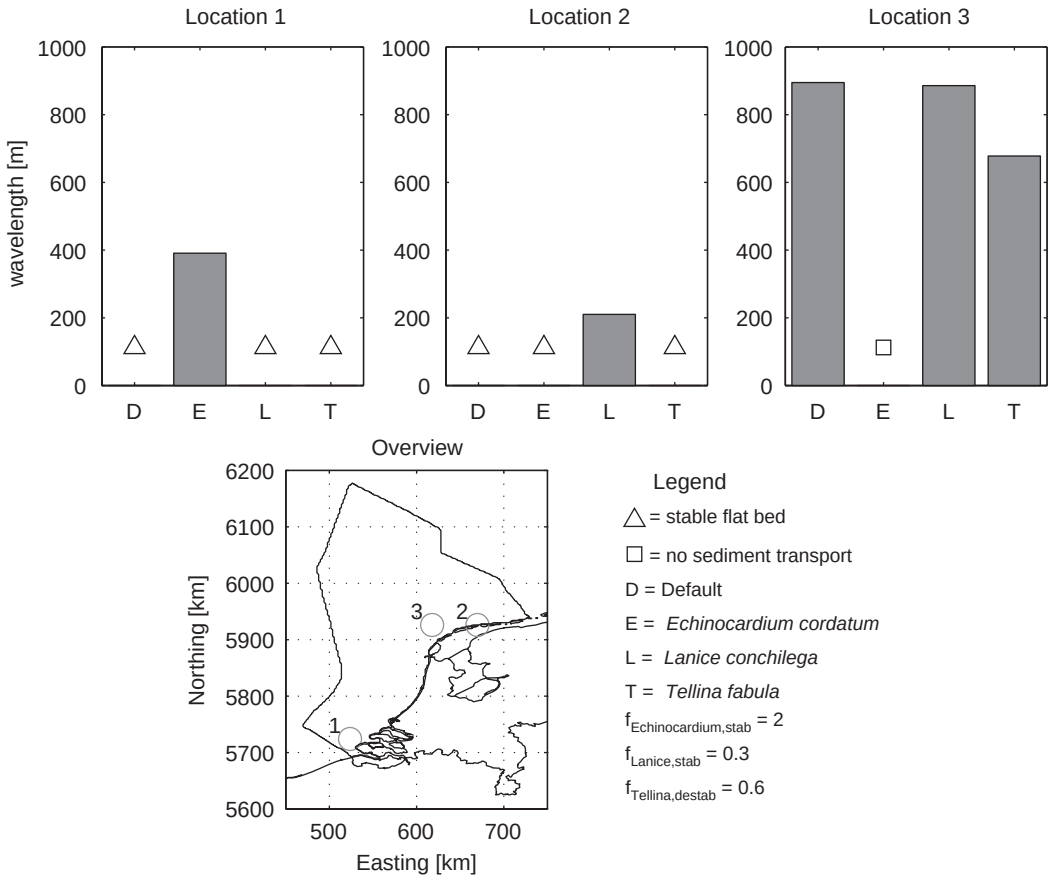

Fig. 8. Model results for the occurrence of bedforms, for three different locations on the Dutch part of the North Sea. Process parameters are shown in Table 2.

between hydrodynamics, geomorphodynamic and biological processes. From the bio-geomorphological loop (i.e., an extension of the morphological loop described by Roos and Hulscher, 2003) it is clear that each of these processes have different temporal and spatial scales (Fig. 9). The separation in three timescales is essential, as the interaction between hydrodynamics, sediment transport and biological processes act within a tidal cycle (half a day) and the bed evolution acts on a much longer time τ (decades to centuries). The time scale on which the biological processes alter is seasonal. However, there are also strong indications that biological processes may differ on a much longer time and spatial scale, for example, due to a northerly shift in geographical distribution of key species as a result of global warming (Widdows and Brinsley, 2002).

Besides, there are also strong indications that a feedback exists from the bed evolution to the biological community and the processes they influence (e.g. Ryan et al., 2007). For example, Daniell et al. (2008) found a relation between the occurrence of seagrass beds on the one hand and dune migration and sand supply on the other hand. In the present model study, we explored a limited but important number of biological effects within the bio-geomorphological feedback loop (i.e., black arrows in Fig. 9). It is an important challenge for the future to extend these kinds of explorations by including both temporal scales plus feedbacks from changes in hydrodynamics, sediment transport and bed evolution to the biological activity (white arrows in Fig. 9). For this purpose, we first need a better parameterization of the biological activity to include in idealized models and good field data sets for model validation.

Validation of the model results is partly feasible by linking the modeled occurrence of bedforms (Fig. 9) with the observed occurrence of bedforms (Fig. 2). However, the presence of biota at the three locations is not explicitly known. Nevertheless, the observed presence of bedforms at location 1 is not in accordance with the default model settings for location 1, suggesting that bio-engineers might be responsible for the occurrence of bedforms at this typical location. As we have no further information, we cannot verify this hypothesis.

It will also be an important challenge to incorporate anthropogenic influences in future model studies, as human activities may strongly affect biological communities (e.g. bottom trawling, foreshore nourishments, sand mining, dredging activities, construction of offshore wind farms). Given the bio-geomorphological influences shown in this paper, seabed morphology could drastically change when benthic species that act as bio-engineers are disturbed by anthropogenic factors. Consequently, we argue that the assessment of human activities on the seabed not only needs to take into account a change in physical processes (e.g. currents, sediment composition, water depth) and the direct influence on the ecosystem, but also the change in biomass of bio-engineering species and thereby on seabed morphology. The model proposed in this paper offers a valuable example and how such problems may be addressed.

6. Conclusions

The Dutch part of the North Sea is not only characterized by different seabed patterns, but also by a diverse biological community. Some bio-engineering species within this benthic community are able to significantly influence the sediment transport processes and hydrodynamics in the North Sea area, and thereby

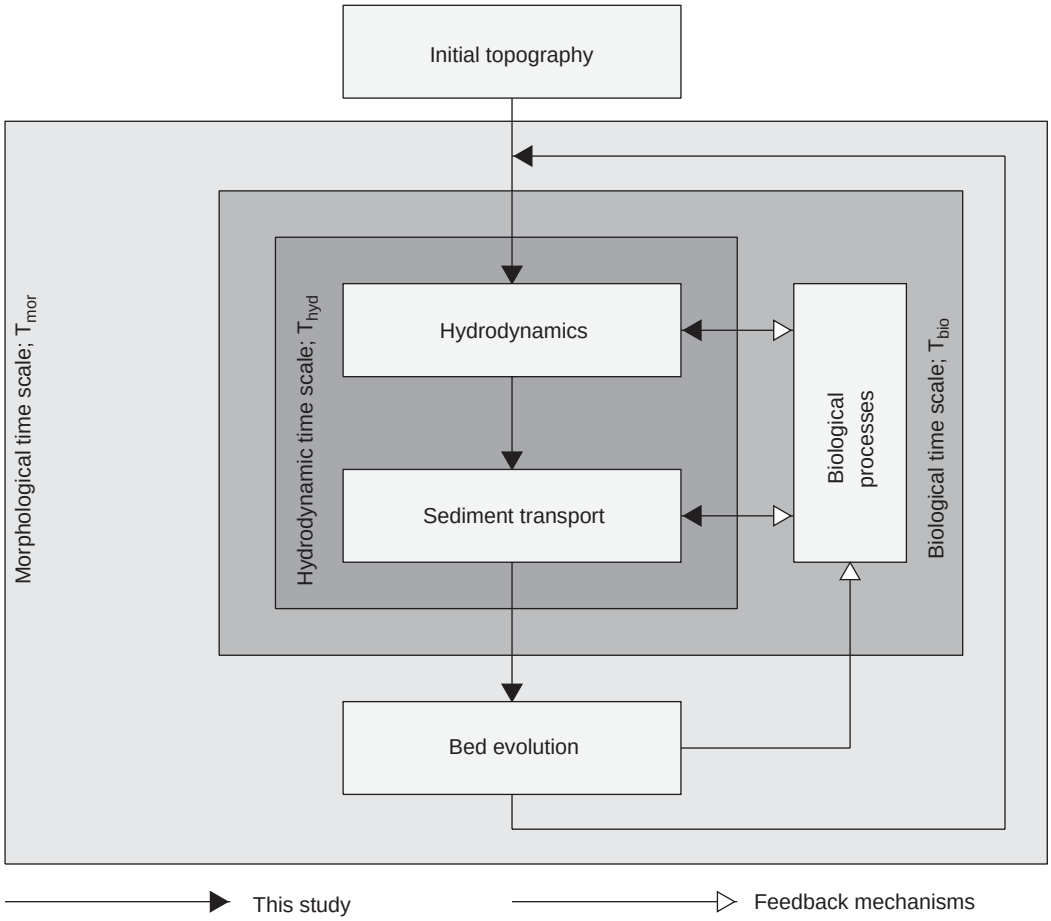

Fig. 9. The bio-morphological loop, which consists of water movement (hydrodynamics), transport of sediment, biological processes and bed evolution. Starting from an initial topography, the water movement initiates the transport of sediment. Both the hydrodynamics and sediment transport are influenced by biota. The fast time scale of the interaction between hydrodynamics, sediment transport and biological processes compared to the slow time scale of bed evolution, allows us to only focus on the tidal average sediment transport. The result is an updated topography, which is the input to start again the computation of the hydrodynamics and sediment transport rates.

have a direct relation to the morphodynamics of the seabed. Firstly, the sea urchin *E. cordatum* feeds from the surface sediment layer and brings fine sediment particles to the deeper sediment and consequently influences the vertical sediment distribution. Secondly, the clam *T. fabula* makes the top layer of the sediment more prone to erosion due to its burrowing and grazing activities. Accordingly, the critical bed shear stress for erosion is reduced. Finally, the tube building worm *L. conchilega* reduces the near-bottom flow and by this facilitates the deposition of fine material. As a result, the ripple height on top of the bedforms is reduced.

By including the maximum likely modification of the transport parameters by these bio-engineers in an idealized sandwave model, an initial insight is given into the bio-geomorphological interactions in offshore seabed patterns. First of all, the wavelength of the bedforms is significantly influenced and even more important: stabilizing bio-engineers are able to preserve a stable flat bed, while the physical conditions suggest bed patterns. Likewise the opposite effect is induced by destabilizing benthos.

Future research should focus on improving the parameterization of biological activity on the sediment transport parameters, and thereby generate a tool to extend current models with both seasonal variations in biological activity and feedbacks from seabed evolution to the composition of the biological community. Moreover, gathering site-specific field data both on physical parameters and biological activity will help to validate the proposed modeling approach.

Acknowledgments

This work is part of the PhD research of the first author, which is supported by the Dutch Technology Foundation STW, applied science division of NWO and the Technology Program of the Dutch Ministry of Economic Affairs. We acknowledge Deltares for providing the physical data for the Dutch part of the North Sea. Moreover, we thank Dr. ir. Denie Augustijn for his valuable comments on the draft of this manuscript. Finally, we acknowledge two anonymous reviewers for their suggestions which improved the readability of the paper enormously. This NIOO publication number 4494.

Appendix A. Bio-sandwave model description

The model by Besio et al. (2006) was constructed by introducing the following dimensionless variables:

$$(x,y,z)=(x^*,y^*,z^*)/h_0^*; \quad (u,v,w)=(u^*,v^*,w^*)/U_0^* \tag{A.1a,b}$$

$$\Omega=\Omega^*/\sigma^*; \quad t=\sigma^*/t^*; \quad p=p^*/\rho^* U_0^* \sigma^* h_0^*; \quad \mathbf{D}=\mathbf{D}^* h_0^*/U_0^* \tag{A.2a–d}$$

where h^*_0 is the local averaged water depth, U^*_0 is the maximum value of the depth-averaged fluid velocity during the tidal cycle, σ^* is the angular frequency of the tide, t^* is time, p^* is the pressure, ρ^* is the fluid density and $\mathbf{D}^*$ is the rate of strain tensor. After introducing the dimensionless variables we arrive at the following

non-dimensional model:

$$\nabla \cdot \mathbf{u} = 0, \tag{A.3}$$

$$\frac{\partial \mathbf{u}}{\partial t} + \hat{r}(\mathbf{u}\cdot\nabla)\mathbf{v} = -\nabla p + \delta^2 \nabla\cdot(\upsilon_T 2\mathbf{D}) - \mathbf{Cor} + \mathbf{g}, \tag{A.4}$$

where the kinematic eddy viscosity υ^*_T is written as the product of $\upsilon^*_{T0}\upsilon_T$. The constant υ^*_{T0} is dimensional and provides the order of magnitude of the eddy viscosity, while $\upsilon_T = \upsilon_T(x,y,z,t)$ is a dimensionless function (of order 1) describing the spatial and temporal variations of the turbulence structure. $\mathbf{u} = (u^*,v^*,w^*)$ is the velocity vector.

The hydrodynamic problem is closed by forcing appropriate boundary conditions and providing the function υ^*_T. Details on the boundary conditions can be found in Besio et al. (2006). The eddy viscosity υ^*_T is assumed to depend on the distance from the bed

$$\upsilon^*_T = k\frac{U^*_0 h^*_0}{C}F(\zeta). \tag{A.5}$$

The function $F(\zeta)(\zeta = z^*/h^*)$ describes the vertical structure of the eddy viscosity and is chosen as suggested by Dean (1974). Further, in (A.5), k is the von Karman constant ($k = 0.41$) and C is the friction factor, defined by Fredsøe and Deigaard (1992)

$$C = 5.75\ \log\frac{10.9h^*_0}{z^*_r}, \tag{A.6}$$

where z^*_r is the roughness size related to the height of the ripples. To calculate the height of the ripples Δ^*_r, the empirical predictor proposed by Soulsby and Whitehouse (2005) is used

$$\Delta^*_r = 202 d^* R_p^{-0.369}, \tag{A.7}$$

where R_p is the Reynolds number of sediment particles

$$R_p = \frac{\sqrt{(\rho^*_s/\rho^* - 1)g^* d^{*3}}}{\nu^*}, \tag{A.8}$$

where ν^* is the kinematic viscosity of water ($\nu^* = 1.10^{-6}\,\mathrm{m^2\,s^{-1}}$ for water at 20 °C). Then, following the suggestion of Van Rijn (1991), z^*_r is fixed equal to Δ^*_r.

The dimensionless bed-load transport (q_{Bx},q_{By}) is modeled according to the relationship proposed by Van Rijn (1991):

$$(q_{Bx},q_{By}) = \frac{0.25}{R_p^{0.2}}\left(\frac{\vec{\theta} - \theta_{cr}}{\theta_{cr}}\right)^{1.5}\left(\frac{\theta_x,\theta_y}{\sqrt{\vec{\theta}}}\right)\mathrm{H}\left(1 - \frac{\theta_{cr}}{\theta_x,\theta_y}\right). \tag{A.9}$$

The Heaviside function H is equal to zero for negative arguments and is equal to 1 for positive arguments. In (A.9), θ_{cr} is the critical Shields parameter below which no sediment moves. θ is equal to $\sqrt{\theta_x^2 + \theta_y^2}$, and the Shields parameter in x and y components are:

$$(\theta_x,\theta_y) = \frac{(\tau^*_x,\tau^*_y)}{(\rho^*_s - \rho^*)g^* d^*}, \tag{A.10}$$

where (τ^*_x,τ^*_y) are the shear stress components, which can easily be evaluated by means of the constitutive law, following the approach proposed by Colombini (2004). The correction of the bed-load transport for the variation in bed topography (q_{Px},q_{Py}) is related to the dimensionless bed-load transport and the local bed slope (Talmon et al., 1995).

The dimensionless suspended-load transport (q_{Sx},q_{Sy}) is calculated by using a standard convection–diffusion equation for the dimensionless sediment concentration $c(x,y,z,t)$. Two boundary conditions impose the dimensionless suspended-sediment concentrations at the bed and at the free surface. The latter states the vanishing of sediment flux normal to the free surface, while the former forces a reference concentration c_a at a distance equal to 0.01 h from the seabed. Following Van Rijn (1991)

$$c_a = 1.5\frac{d}{R_p^{0.2}}\left(\frac{\vec{\theta} - \theta_{cr}}{\vec{\theta}}\right)^{3/2}, \tag{A.11}$$

where d is the dimensionless grain size $d = d^*/h^*_0$.

The total dimensionless sediment transport (q_{Tx},q_{Ty}) is

$$(q_{Tx},q_{Ty}) = (q_{Bx},q_{By}) + (q_{Px},q_{Py}) + (q_{Sx},q_{Sy}). \tag{A.12}$$

Bed level changes can be calculated by a sediment continuity equation, which in dimensionless form is

$$\frac{\partial h}{\partial T} = \frac{\partial q_{Tx}}{\partial x} + \frac{\partial q_{Ty}}{\partial y}. \tag{A.13}$$

Relation (A.13) simply states that convergence (or divergence) of the sediment flux must be accompanied by a rise (or fall) of the bed profile.

References

Andersen, T.J., Jensen, K.T., Lund-Hansen, L., Mouritsen, K.N., Pejrup, M., 2002. Enhanced erodibility of fine-grained marine sediments by *Hydrobia ulvae*. Journal of Sea Research 48, 51–58.

Austen, I., Andersen, T.J., Edelvang, K., 1999. The influence of benthic diatoms and invertebrates on the erodibility of an intertidal mudflat, the Danish Wadden Sea. Estuarine, Coastal and Shelf Science 49, 99–111.

Baptist, M.J., van Dalfsen, J., Weber, A., Passchier, S., van Heteren, S., 2006. The distribution of macrozoobenthos in the Southern North Sea in relation to meso-scale bedforms. Estuarine, Coastal and Shelf Science 68, 538–546.

Baumfalk, Y.A., 1979. Heterogeneous grain size distribution in tidal flat sediment caused by bioturbation activity of *Arenicola marine* (polychaeta). Netherlands Journal of Sea Research 13, 428–440.

Besio, G., Blondeaux, P., Vittori, G., 2006. On the formation of sandwaves and sand banks. Journal of Fluid Mechanics 557, 1–27.

Besio, G., Blondeaux, P., Brocchini, M., Hulscher, S.J.M.H., Idier, D., Knaapen, M.A.F., Németh, A.A., Roos, P.C., Vittori, G., 2008. The morphodynamics of tidal sandwaves: a model overview. Coastal Engineering 55, 657–670.

Borja, A., Franco, J., Pérez, V., 2000. A marine biotic index to establish the ecological quality of soft-bottom benthos within European estuarine and coastal environments. Marine Pollution Bulletin 12, 1100–1114.

Borsje, B.W., De Vries, M.B., Hulscher, S.J.M.H., De Boer, G.J., 2008a. Modeling large scale cohesive sediment transport with the inclusion of biological activity. Estuarine, Coastal and Shelf Science 78, 468–480.

Borsje, B.W., Besio, G., Blondeaux, P., Hulscher, S.J.M.H., Vittori, G., 2008b. Exploring biological influence on offshore sandwave length. Marine and River Dune Dynamic III, International Workshop, April 1–3 2008, Leeds. Parsons D.R., Garlan T., Best J.L. (Eds), pp 31-38.

Bouma, T.J., van Duren, L.A., Temmerman, S., Claverie, T., Blanco-Garcia, A., Ysebaert, T., Herman, P.M.J., 2007. Spatial flow and sedimentation patterns within patch of epibenthic structures: combining field, flume and modeling experiments. Continental Shelf Research 27, 1020–1045.

Burone, L., Muniz, P., Pires-Vanin, A.M.S., Rodrigues, M., 2003. Spatial distribution of organic matter in the surface sediments of Ubatuba Bay (southeastern Brazil). Annals of the Brazilian Academy of Sciences 75, 77–90.

Cherlet, J., Besio, G., Blondeaux, P., van Lancker, V., Verfaillie, E., Vittori, G., 2007. Modeling sandwave characteristics on the Belgian Continental Shelf and in the Calais-Dover Strait. Journal of Geophysical Research 112, C06002.

Colombini, M., 2004. Revisiting the linear theory of sand dune formation. Journal of Fluid Mechanics 502, 1–16.

Cramer, A., Duineveld, G.C.A., Jenness, M.I., 1991. Observations on spatial distribution, metabolism and feeding strategy of *Echinocardium cordatum* (Pennant) (Echinodermata) and the implications for its energy budget. In: Cramer, A., (Ed.), Benthic Metabolic Acitivy at Frontal Systems in the North Sea. Ph.D. Thesis, University of Amsterdam, Amsterdam, pp. 63–74.

Daniell, J.J., Harris, P.T., Hughes, M.G., Hemer, M., Heap, A., 2008. The potential impact of bedform migration on seagrass communities in Torres Strait, northern Australia. Continental Shelf Research 28, 2188–2202.

De Deckere, E.M.G.T., Tolhurst, T.J., De Brouwer, J.F.C., 2001. Destabilization of cohesive intertidal sediments by infauna. Estuarine, Coastal and Shelf Science 53, 665–669.

Dean R.B., 1974. AERO Report 74-11. Imperial College, London.

Degraer, S., Verfaillie, E., Willems, W., Adriaens, E., Vincx, M., Van Lancker, V., 2008. Habiat suitability modelling as a mapping tool for macrobenthic communities: An example from the Belgian part of the North Sea. Continental Shelf Research 28, 369–379.

Dodd, N., Blondeaux, P., Calvete, D., De Swart, H., Falques, A., Hulscher, S.J.M.H., Rozynski, G., Vittori, G., 2003. The use of stability methods for understanding the morphodynamical behaviour of coastal systems. Journal of Coastal Research 19, 849–865.

Dyer, K.R., Huntley, D.A., 1999. The origin, classification and modeling of sandbanks and ridges. Continental Shelf Research 19, 1285–1330.
Eckman, J.E., Nowell, A.R.M., Jumars, P.A., 1981. Sediment destabilization by animal tubes. Journal of Marine Research 39, 361–374.
Featherstone, R.P., Risk, M.J., 1977. Effects of tube-building polychaetes on intertidal sediments of the Minas Basin, Bay of Fundy. Journal of Sedimentary Petrology 47, 446–450.
Fredsøe, Deigaard (Eds.), 1992. Mechanics of Coastal Sediment Transport. Advance Series on Ocean Engineering. World Scientific, Singapore xviii+369 p.
Friedrichs, M., Graf, G., Springer, B., 2000. Skimming flow induced over a simulated polychaete tube lawn at low population densities. Marine Ecology Progress Series 192, 219–228.
Gilbert, F., Hulth, S., Grossi, V., Poggiale, J.-C., Desrosiers, G., Rosenberg, R., Gerino, M., Francois-Carcaillet, F., Michaud, E., STora, G., 2007. Sediment reworking by marine benthic species from the Gullmar Fjord (Western Sweden): importance of faunal biovolume. Journal of Experimental Marine Biology and Ecology 348, 133–144.
Heip, C., Basford, D., Craeymeersch, J.A., Dewarumez, J.-M., Dörjes, J., De Wilde, P., Duineveld, G., Eleftheriou, A., Herman, P.M.J., Niermann, U., Kingston, P., Künitzer, A., Rachor, E., Rumohr, H., Soetaert, K., Soltwedel, T., 1992. Trends in biomass, density and diversity of North Sea macrofauna. Journal of Marine Science 49, 13–22.
Holthe, T., 1986. Polychaeta Terebellomorpha. Marine invertebrates of Scandinavia, No. 7. Norwegian University Press, Oslo, 194 pp.
Hulscher, S.J.M.H., 1996. Tidal-induced large-scale regular bed form patterns in a three-dimensional shallow water model. Journal of Geophysical Research C9 (101), 20727–20744.
Hulscher, S.J.M.H., Van den Brink, G.M., 2001. Comparison between predicted and observed sandwaves and sandbanks in the North Sea. Journal of Geophysical Research 106 (C5), 9327–9338.
Huthnance, J., 1982. On one mechanism forming linear sandbanks. Estuarine Coastal Shelf Science 14, 79–99.
Knaapen, M.A.F., Holzhauer, H., Hulscher, S.J.M.H., Baptist, M.J., De Vries, M.B., Van Ledden, M., 2003. On the modelling of biological effects on morphology in estuaries and seas. In: Sánchez-Arcilla, A., Bateman, A. (Eds.), Proceedings of the Third IAHR Symposium on River, Coastal and Estuarine Morphodynamics Conference. IAHR, Barcelona, Spain, pp. 773–783.
Künitzer, A., Duineveld, G.C.A., Basford, D., Dewarumez, J.-M., Dörjes, J., Eleftheriou, A., Heip, C., Herman, P.M.J., Kingston, P., Niermann, U., Rumohr, H., De Wilde, P.A.W.J., 1992. The benthic infauna of the North Sea: species distribution and assemblages. Journal of Marine Science 49, 127–143.
Lohrer, A.M., Thrush, S.F., Hunt, L., Hancock, N., Lundquist, C., 2005. Rapid reworking of subtidal sediments by burrowing spatangoid urchins. Journal of Experimental Marine Biology and Ecology 321, 155–169.
Lumborg, U., Andersen, T.J., Pejrup, M., 2006. The effect of *Hydrobia ulvae* and microphytobenthos on cohesive sediment dynamics on an intertidal mudflat described by means of numerical modeling. Estuarine, Coastal and Shelf Science 68, 208–220.
Mortensen, T., 1927. Handbook of the Echinoderms of the British Isles. Oxford University Press, Oxford, 471 pp.
McCave, I.N., 1971. Sandwaves in the North Sea off the coast of Holland. Marine Geology 10, 199–225.
Németh, A.A., Hulscher, S.J.M.H., De Vriend, H.J., 2003. Offshore sandwave dynamics, engineering problems and future solutions. Pipeline and Gas Journal 230, 67–69.
O'Donoghue, T., Doucette, J.S., van der Werf, J.J., Ribberink, J.S., 2006. The dimensions of sand ripples in full-scale oscillatory flows. Coastal Engineering 53, 997–1012.
Orvain, F., Sauriau, P., Bacher, C., Prineau, M., 2006. The influence of sediment cohesiveness on bioturbation effects due to *Hydrobia ulvae* on the initial erosion of intertidal sediments: A study combining flume and model approaches. Journal of Sea Research 55, 54–73.
Osinga, R., Kop, A.J., Malschaert, J.F.P., Van Duyl, F.C., 1997. Effects of the sea urchin *Echinocardium cordatum* on bacterial production and carbon flow in experimental benthic systems under increasing organic loading. Journal of Sea Research 37, 109–121.
Paarlberg, A.J., Knaapen, M.A.F., de Vries, M.B., Hulscher, S.J.M.H., Wang, Z.B., 2005. Biological influences on morphology and bed composition of an intertidal flat. Estuarine, Coastal and Shelf Science 64, 577–590.
Rabaut, M., Guilini, K., Van Hoey, G., Vincx, M., Degraer, S., 2007. A bio-engineered soft-bottom environment: the impact of *Lanice conchilega* on the benthic species-specific densities and community structure. Estuarine, Coastal and Shelf Science 75, 525–536.
Roos, P.C., Hulscher, S.J.M.H., 2003. Large-scale seabed dynamics in offshore morphology: modeling human intervention. Reviews of Geophysics 41 (2), 1010.
Ryan, D.A., Brooke, B.P., Collins, L.B., Kendrick, G.A., Baxter, K.J., Bickers, A.N., Siwabessy, P.J.W., Pattiaratchi, C.B., 2007. The influence of geomorphology and sedimentary processes on shallow-water benthic habitat distribution: Esperance Bay, Western Australia. Estuarine, Coastal and Shelf Science 72, 379–386.
Soulsby, R.L., 1983. The bottom boundary layer of shelf seas. In: Johns, B. (Ed.), Physical Oceanography of Coastal and Shelf Seas. Elsevier Science, New York, pp. 189–266.
Soulsby, R.L., Whitehouse, R.J.S., 2005. Prediction of ripples properties in shelf seas: Mark 2 predictor for time evolution. Rep. TR 154, HR Wallingford Ltd., Wallingford, UK.
Talmon, A.M., Struiksma, N., Van Mierlo, M.C.L.M., 1995. Laboratory measurements of the direction of sediment transport on transverse alluvial bed slopes. Journal of Hydraulic Research 33, 495–517.
Tebble, N., 1966. British bivalve seashells. British Museum (Natural History). London, 212 pp.
Van Duren, L.A., Herman, P.M.J., Sandee, A.J.J., Heip, C.H.R., 2006. Effects of mussel filtering activity on boundary layer structure. Journal of Sea Research 55, 3–14.
Van Leeuwen, B., Augustijn, D.C.M., van Wesenbeeck, B.K., Hulscher, S.J.M.H., de Vries, M.B., 2008. Modeling mussel bed influence on fine sediment dynamics on a Wadden Sea intertidal flat. Proceedings BioGeoCivil Engineering Conference 23–25 June 2008, Delft, the Netherlands, p. 90–98.
Van Rijn, L.C., 1991. Sediment transport in combined waves and currents, in Proceedings of Euromech 262, Balkema, A.A., Brookfield, VT.
Widdows, J., Brinsley, M.D., Bowley, N., Barrett, C., 1998. A benthic annular flume for in situ measurement of suspension feeding/biodeposition rates and erosion potential of intertidal cohesive sediments. Estuarine, Coastal and Shelf Science 56, 27–38.
Widdows, J., Brinsley, M.D., Salkeld, P.N., Lucas, C.H., 2000. Influence of biota on spatial and temporal variation in sediment erodability and material flux on a tidal flat (Westerschelde, The Netherlands). Marine Ecology Progress Series 194, 23–37.
Widdows, J., Brinsley, M.D., 2002. Impact of biotic and abiotic processes on sediment dynamics and the consequences to the structure and functioning of the intertidal zone. Journal of Sea Research 48, 143–156.